


RESEARCH

Open Access



Study on Mechanical Properties of Polycaprolactone Modified Cement-Based Material

Hai-feng Lu^{1,2*} , Kai Zhang¹, Jin-long Yi¹ and Ai-chao Wei¹

Abstract

With the continuous development of economy, engineering construction is developing towards deep high-stress area, and the problems of large-deformation engineering are becoming more and more serious. Anchoring grouting is a very effective support reinforcement method. The anchoring grouting materials used in the project are mainly cement paste and cement mortar. The characteristics of the grouting material have a decisive influence on the grouting effect. However, it is difficult for the existing grouting materials to satisfy the requirements of strength and deformation at the same time, and improvement is urgently needed. Polycaprolactone (PCL) is an organic polymer material of good engineering properties, including high ductility, good stability and strong impact resistance. In this paper, PCL was added as an auxiliary additive to cement-based materials innovatively, and the mechanical test and micro-test of PCL-cement-based materials were carried out. The results show that adding PCL can significantly increase the compressive strength of cement paste. By adjusting the content of PCL, the strength and ductility of cement mortar can be effectively improved. When the content of PCL is 15%, ideal high performance cement mortar material can be obtained. Anchor grouting is a very effective reinforcement and support method.

Keywords: polycaprolactone (PCL), cement paste, cement mortar, concrete, uniaxial compression test, microscopic test

1 Introduction

With the continuous development of engineering technology and economy, engineering construction is advancing to deep high-stress areas, and various complex geological environments have brought new difficulties and challenges to the construction of engineering facilities (Sha et al., 2015). In deep areas with high tectonic stress and complex tectonic movement history, there are a large number of fracture-loaded strata formed by the mutual cutting of joints and bedding planes (Liu et al., 2008). When excavating and constructing roadways

(or tunnels) in this type of formation, the roadways are prone to large deformations under huge surrounding rock loads, which will greatly affect the safety of the roadway construction and the construction progress (Fig. 1). Therefore, it is of great practical significance to study and solve the problem of large deformation when deep roadways pass through fractured rock masses, and at present, the problem is also a major and difficult issue that needs to be solved urgently in tunnel engineering (Li et al., 2016).

Anchoring grouting is an important method to improve the self-carrying capacity of surrounding rock. It can elevate the overall performance of the fractured rock mass through reinforcement, so that the internal stress of the surrounding rock can be released in a stable and controllable manner, and the surrounding rock load of the supporting structure can be reduced when it

*Correspondence: luhaifeng@whu.edu.cn

¹ School of Civil Engineering, Wuhan University, Wuhan 430072, Hubei, China

Full list of author information is available at the end of the article

Journal information: ISSN 1976-0485 / eISSN 2234-1315



Fig. 1 Rupture-bulking and large deformation of deep surrounding rock.

finally reaches a stable state (Barton & Choubey, 1977; Li et al., 2021). Since the introduction of grouting technology, the research and development work on grouting materials has never stopped (Bruce et al., 1999). In the 1850s, the British W. R. kiniple first used cement grout as a grouting material when reinforcing the foundation of the spillway of a reservoir, which effectively improved the bearing capacity of the foundation (Du, 2018). In the past 200-year-development of grouting technology, cement-based grouting material has become the first choice in the field of crack grouting reinforcement due to its convenient configuration, good injectability, and high strength of its induration (Du et al., 2017; Qing et al., 2021; Zhao et al., 2015). With the vigorous development of infrastructure construction in western China and the proposal of “Deep Resources Exploration and Mining” strategy, traditional cement grouting materials cannot satisfy the requirements for strength and deformation performance when faced with the complex construction conditions in deep high-stress fractured geological zones (Liu et al., 2019). For example, diversion tunnels of hydropower projects, deep geological storage of nuclear waste, and deep coal mining projects with a depth of more than one thousand meters. The buried depth of Wushaoling tunnel, which was completed in 2006, is 450–1100 m. When it passed through the regional large fault fracture zone in the Qilian Mountains, the initial support of the tunnel was severely deformed, with the maximum deformation reaching 1200 mm and the maximum deformation rate up to 168 mm/d, bringing huge challenges to the construction (Li & Zhu, 2008). The Maoxian Tunnel on the Chengdu–Lanzhou Railway, located in the fault zone of Longmen Mountains, has a maximum buried depth of about 1656 m. As the strata that the tunnel passes are mainly carbonaceous phyllite and limestone, and the folds, faults and joints of the rock mass are densely developed, the tunnel lies in a typical high crustal stress fractured geological zone. During the construction process, it

encountered long-term, continuous large deformations, and the maximum deformation even exceeded 1000 mm. Traditional grouting materials cannot deal with such large deformation of surrounding rock (Yang, 2009). Through the above engineering examples, it can be seen that in the face of complex geological conditions such as large buried depth, large cross section, and high crustal stress, traditional cement-based grouting materials still have a series of shortcomings, including low consolidated strength, negligible tensile strength of joints after grouting, and poor resistance to large deformations (Lu et al., 2021; Wang et al., 2007). Support and reinforcement engineering has put forward higher requirements for mechanical properties of traditional cement grouting materials (Guan et al., 2020). At the same time, research on the modification of cement-based materials is also in full swing.

In the 1930s, scientists used ϵ -caprolactone monomer to prepare polycaprolactone (PCL) polymer materials for the first time by cyclic polymerization in the presence of initiators. As PCL is a non-toxic and harmless material with microbial degradability, good stability and biocompatibility (Abbah et al., 2009), it has been especially widely used in the medical field since its invention to the 1980s and 1990s. For example, it is utilized as a drug delivery carrier, surgical sutures, medical dressings, orthopedic fixation devices, etc. (Ajili et al., 2009; Alani et al., 2009); meanwhile, it is also widely used in plastic packaging and tissue engineering (Kumar et al., 2020; Li et al., 2020). In the twenty-first century, people have noticed the excellent rheological and viscoelastic characteristics of PCL, which is very conducive to processing and can be formed at low temperatures. In addition, the crystallinity of PCL is strong, its crystalline state has high strength at room temperature, and the viscosity of its molten state is relatively large (Chen et al., 2015). The above-mentioned excellent engineering properties of PCL have quickly attracted the attention of materials

scientists. According to research, the appearance of PCL is milky white with a waxy texture, the melting point is about 60 °C, and the molecules contain freely rotatable C–O bonds and C–C bonds, which makes PCL have good flexibility and processability in terms of macroscopic material properties, and can be extruded, injection molded, wire drawn, blown film, etc. (Woodruff & Hutmacher, 2010). Relevant scholars have heated the PCL sample to the melting point, and then rapidly cooled it to a predetermined crystallization temperature. The result reveals that the crystallization process of PCL is roughly the formation of needle-shaped crystals, columnar crystals, approximately elliptical-shaped crystals, and finally a large spherulite in contact with the entire sample crystal phase (Han et al., 2011). In addition, PCL has good thermal stability; its decomposition temperature is higher than other esters, which is about 350 °C. Its mechanical properties are similar to those of polyolefin (Leonés et al., 2020), with the tensile strength being about 12–30 MPa, and the elongation at break reaching 300–600%.

Compared with traditional silicate building materials, PCL shows excellent ductility and higher strength. Its good mechanical properties and workability can make up for the lack of related properties of grouting reinforcement materials in geotechnical engineering. However, there are still few studies and reports on the application of PCL in this field. To meet the above engineering requirements, the physical and mechanical characteristics and microstructures of PCL are studied and analyzed in this paper. It is found that PCL has compact internal structure, good ductility, high strength and excellent engineering performance. By adjusting the mix ratio and adding PCL as ductile additive to the cement slurry, the mechanical properties and microstructure of PCL-cement-based materials are further investigated in this paper, which aims to provide a scientific basis for the research and design of anchoring grouting materials and high-strength and high-toughness concrete.

2 Sample Preparation and Experiments

2.1 Sample Preparation

2.1.1 Materials

1. Ordinary Portland Cement: The P.O42.5 Ordinary Portland Cement produced by Huaxin Cement Plant

was used, and all indicators were in line with the standard “General Portland Cement” (GB175-2007).

2. Polycaprolactone: A synthetic polyester biopolymer material with a melting point of about 60 °C was used, showing higher viscosity and poor fluidity in the molten state. The PCL used in the experiment was a powdered solid. After mixing it with cement-based raw materials, the powdered PCL can be more evenly distributed in the cement and sand particle system. The technical indexes of PCL used in this paper are as follows (Table 1):
3. Sand: China ISO standard sand was used for the preparation of cement mortar.
4. Water: Tap water was adopted.

2.1.2 Instruments for Sample Preparation

(1) A small mixing equipment; (2) a set of detachable steel cylindrical molds with an inner diameter of 50 mm and a height of 100 mm; (3) a set of detachable steel cube molds with a size of 20 mm × 20 mm × 20 mm; (4) an electronic balance (with weighing accuracy 0.1 g); (5) a digital display thermostat water bath (temperature range is from room temperature to 100 °C); (6) a barrel of lubricating oil; (7) a stainless steel plate, a plastic glue bucket, a hammer, a screwdriver, a spoon, a putty knife, etc.

2.1.3 PCL Sample Preparation

To study the physical and mechanical properties of the PCL, a standard cylindrical mold with an inner diameter of 50 mm and a height of 100 mm was used to hold a sufficient amount of PCL granules, which was later heated and melted in a water bath heater at 70 °C, and then taken out. After hardening, cooling and demolding, a standard PCL cylindrical sample was obtained. The specific process is shown in Fig. 2. The heating and melting process of the PCL granules lasted about 2.5 h, and the crystal hardening process was about 0.5 h. After cooling, the sample was demolded after being heated in the water bath for 24 h.

As the particle sizes of the PCL granules was large, the melting process in the water bath was slow and it was difficult to uniformly mix them into the cement-based slurry; therefore, the PCL added to the composite cement-based material was in powder form.

Table 1 Basic technical indicators of PCL.

PCL model	Molecular formula	Approximate molecular weight	Appearance	Particle size (μm)	Hydroxyl value (mg KOH/g)	Melt index	Melting point range (°C)	Sample density (g/cm ³)
Capa 6500	(C ₆ H ₁₀ O ₂) _n	50,000	Grain	3000	2	7	58–60	1.073
Capa 6506	(C ₆ H ₁₀ O ₂) _n	50,000	Powder	3–6	2	7	58–60	1.086

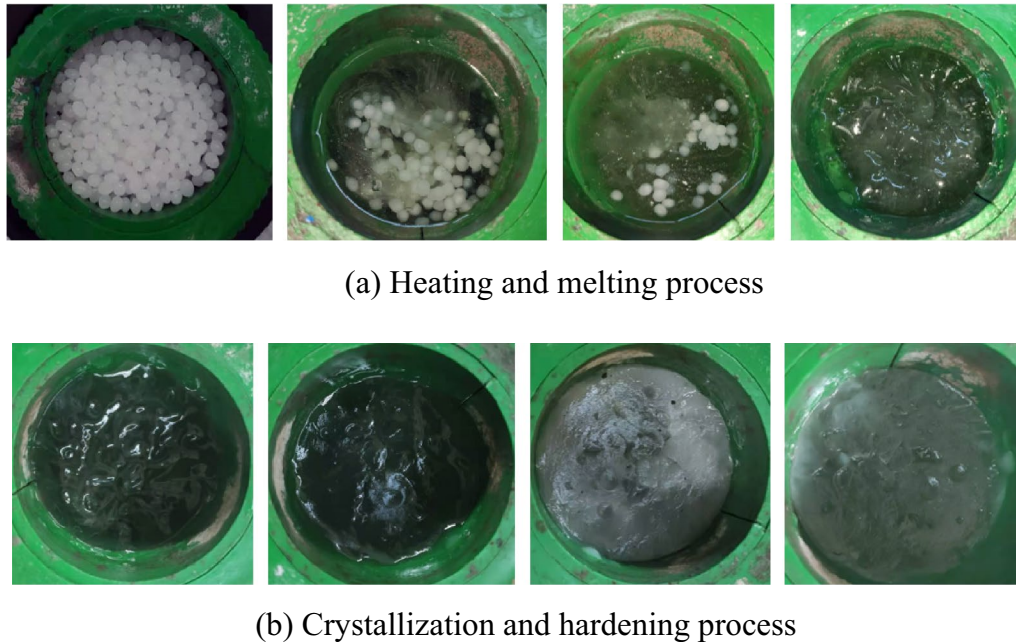


Fig. 2 Sample preparation of PCL granules.

This experiment also included a set of standard cubic samples made of PCL powder, with a size of $20\text{ mm} \times 20\text{ mm} \times 20\text{ mm}$. Since the sample volume was small and the powdery form could be fully heated, the melting process of PCL powder in water bath was only 30 min and the hardening time was shorter compared to that of PCL granules. The sample was also demolded after 24 h. Fig. 3a shows the morphology of the PCL powder during the cooling and crystallization process, and Fig. 3b shows the image of prepared PCL powder sample.

2.1.4 Preparation of PCL-Cement Paste Sample

PCL does not have cohesiveness at room temperature. In this paper, a water bath heating method was adopted to incorporate PCL into cement-based materials. Among

them, the mix design and sample preparation process of the PCL-cement paste sample were as follows:

- (1) Cement paste mix design: Based on the commonly used grout mix design scheme at the grouting site, the cement paste water–cement ratio (W/C) was set to 0.8. The PCL powder was used as an additive, and its mass accounted for 0.0%, 0.9% and 1.8% that of the cement, respectively. Then, the mixture was poured into the prepared pure cement slurry and stirred evenly.
- (2) Sample moulding: The mold shall be cleaned before pouring, and its inner wall shall be evenly coated with a layer of lubricating oil. The evenly mixed PCL cement paste was poured into the standard

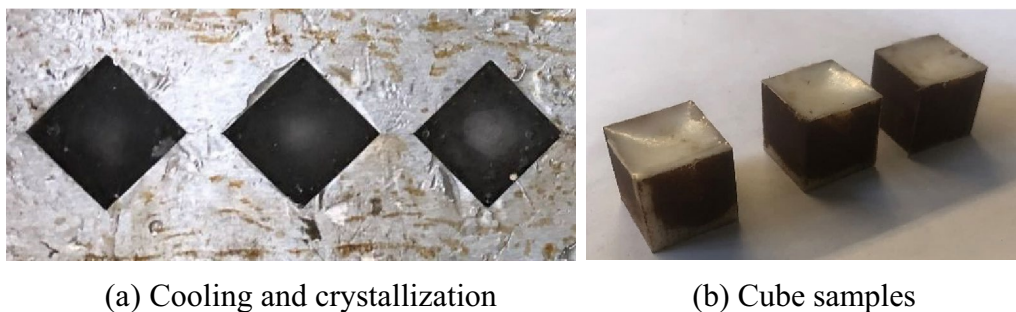


Fig. 3 Sample preparation of PCL powder.

cylindrical mold with an inner diameter of 50 mm and a height of 100 mm. The vibration table or manual vibration method was used in the pouring process to ensure that the cement paste and PCL powder were evenly mixed. After pouring, a scraper was used to gently scrape and smooth the slurry that was higher than the test mold. For each group of samples, three identical test blocks were poured and numbered.

- (3) Water bath heating: The mold containing the paste was placed in a water bath and heated for 30 min (as shown in Fig. 4a). The temperature of the water bath used in the test was 70 °C, slightly higher than the melting point of PCL. After cooling, the PCL powder could fill and cement the stone, achieving an effect similar to grouting reinforcement. At the same time, the non-heating group 1–1 was set as a control.
- (4) Curing, molding and demolding: After the water bath treatment, the paste was placed in a curing box or an indoor environment with a suitable temperature (as shown in Fig. 4b) for 7 days of curing. Demoulding should be carefully operated to prevent sample damage. The specific mixing ratio and conditions for sample preparation are shown in Table 2:

2.1.5 PCL-Cement Mortar Sample Preparation

1. Cement mortar mix design: The water–cement ratio (W/C) of cement mortar sand was set to 0.6, and the mass of the standard sand added was 3 times that of the cement. Considering PCL as auxiliary additive

Table 2 Cement paste mix design and preparation conditions.

No.	Water–cement ratio (W/C)	PCL content/% (PCL/C)	Water bath temperature/°C	Water bath time/min	Curing time/d
1–1	0.8	0.0	0	0	7
1–2	0.8	0.0	70	30	7
1–3	0.8	0.9	70	30	7
1–4	0.8	1.8	70	30	7

and not constituting the main component of cementitious material, the influence of PCL on the mechanical properties of cement mortar is studied. The PCL mass was set as 1%, 2%, 3%, 5%, 10%, 15%, 20% of the cement mass. At the same time, to verify that the PCL can play a better cementation effect and has good toughness, the experiment designed comparative groups 2–9. The preparation process consists of mixing PCL and standard sand evenly, melting PCL by heating and forming homogeneous samples after cooling. The PCL-sand sample is shown in Fig. 5a.

2. Sample molding: The well-mixed PCL-cement mortar sample was poured into a detachable steel cube mold with a size of 20 mm × 20 mm × 20 mm. Three identical blocks were poured for each group of samples.
3. Water bath heating: Theoretically, when the initial setting process of cement was basically finished and the cement mortar was in the initial stage of hardening, the PCL powder should be cooled and hardened at the same time, so that it could cement the mortar aggregates. Therefore, the water bath heating was performed after the initial setting process was over (about 45 min of pouring) (as shown in Fig. 5b).

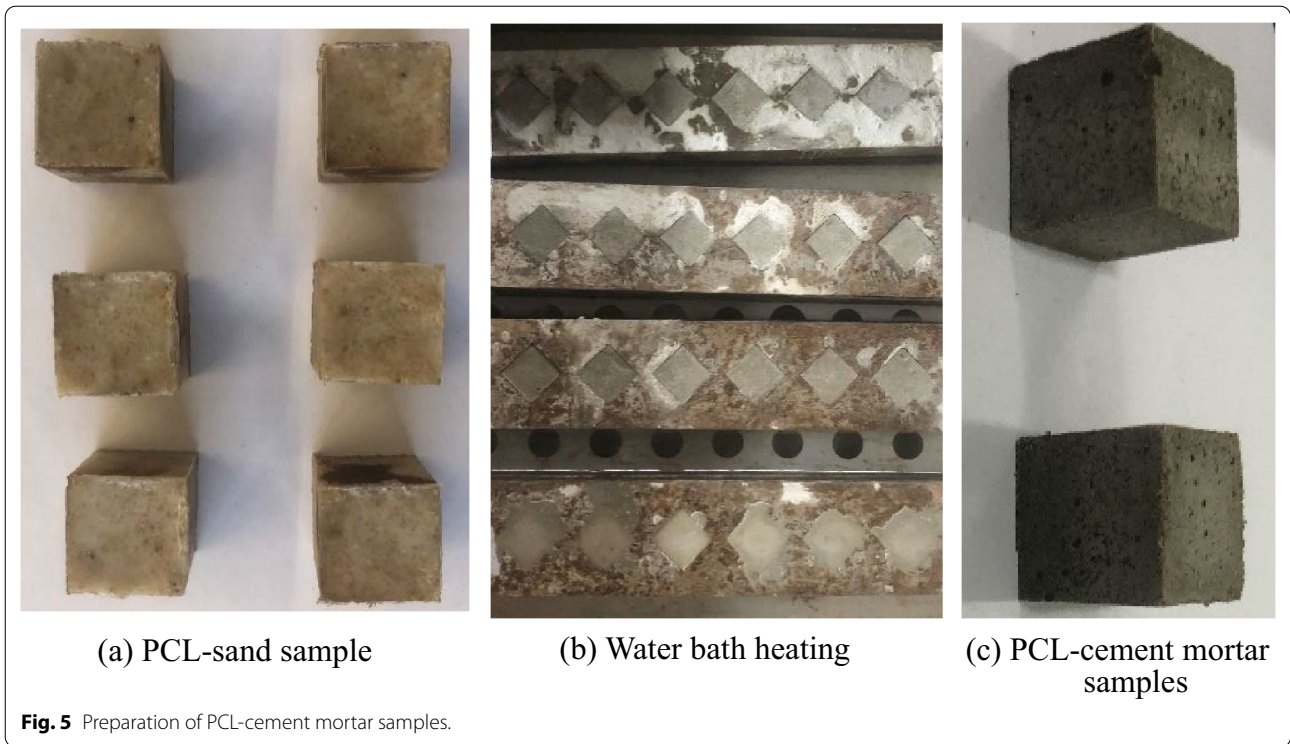


(a) Water bath heating



(b) Curing and molding

Fig. 4 Preparation of PCL-cement paste samples.



4. Curing, molding and demolding: The curing time of each group of samples was 28 days, after which the samples were demolded, as shown in Fig. 5c. The specific mix design and sample preparation conditions of PCL-cement mortar samples are shown in Table 3.

2.2 Methods and Instruments

To study the properties of PCL modified cement-based materials, the mechanical properties and microstructures of PCL specimens, PCL-cement paste specimens,

and PCL-cement mortar specimens were tested by experiments.

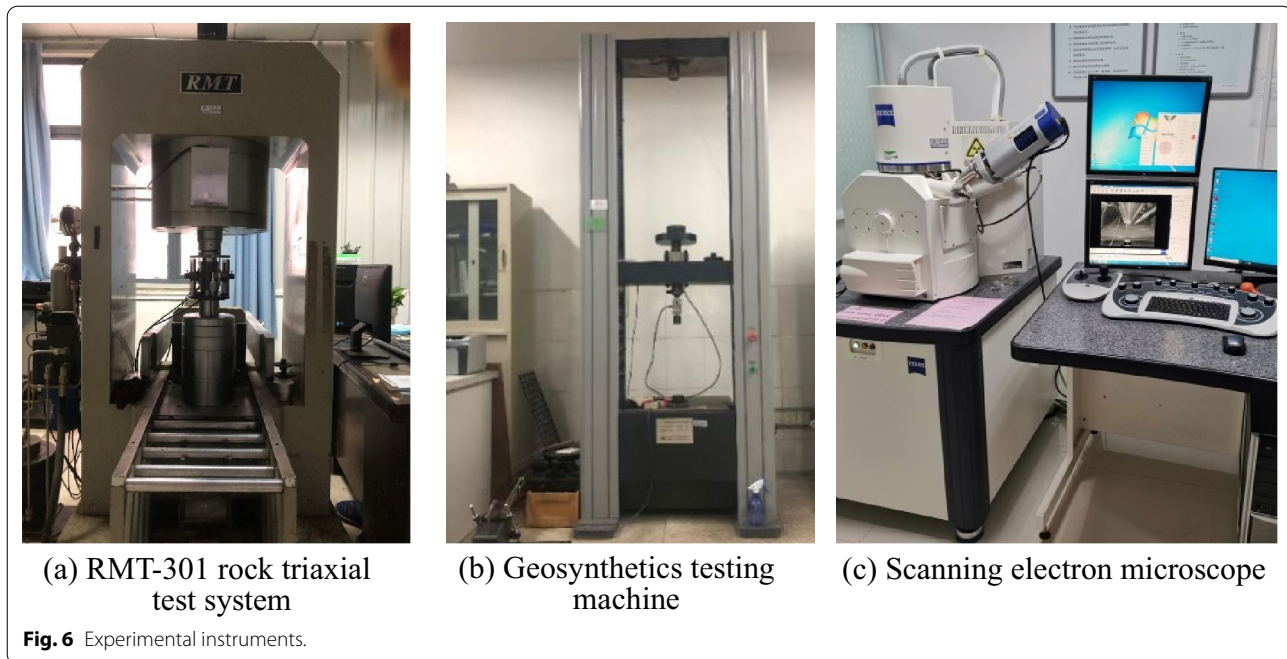
2.2.1 Compression Test of PCL Specimens

In this paper, an RMT-301 rock direct shear/triaxial compression combined testing machine was used to test the compressive strength of the PCL samples (as shown in Fig. 6a). The PCL sample size for uniaxial compression test was 20 mm × 20 mm × 20 mm, and the loading rate was controlled by strain to 0.5 mm/min.

After the uniaxial compression test was performed on the PCL sample, it was found that the plastic characteristics were obvious, and the compression curve had no

Table 3 PCL-cement mortar samples mix design.

No.	Water (W)	Cement (C)	Standard sand (S)	PCL content/%	Water bath temperature/°C	Water bath time/min	Curing time /d
2-1	0.6	1	3	0	70	30	28
2-2	0.6	1	3	1	70	30	28
2-3	0.6	1	3	2	70	30	28
2-4	0.6	1	3	3	70	30	28
2-5	0.6	1	3	5	70	30	28
2-6	0.6	1	3	10	70	30	28
2-7	0.6	1	3	15	70	30	28
2-8	0.6	1	3	20	70	30	28
2-9	0	0	1	60	70	30	28



peak points. According to the standard test method for the compression properties of rigid foams, the compressive strength without yield point was defined as the stress at 10% deformation. Compressive modulus of elasticity was defined as the tangent modulus within the proportional limit of the stress–strain curve. The basic mechanical index of the sample was calculated as follows:

Compressive strength σ_m (MPa):

$$\sigma_m = \frac{P_c}{A_0},$$

where σ_m is the uniaxial compressive strength/MPa; P_c is the maximum compressive force when the relative deformation $\varepsilon < 10\%$ of the specimen/N; A_0 is the initial cross-sectional area of the test piece/mm².

Compression modulus of elasticity E (MPa):

$$E = \sigma_e \times \frac{h_0}{x_e},$$

$$\sigma_e = \frac{F_e}{A_0},$$

where F_e is the compressive force within the proportional limit (there is an obvious straight part in the force–displacement curve)/N; x_e is the compression deformation at F_e /mm; h_0 is the initial thickness of the sample/mm.

2.2.2 Compression Test of PCL-Cement-Based Materials

After the PCL-cement-based specimens were molded, they were cured at room temperature for about 24 h and demolded, and then continued to be cured at room temperature to the specified time. The room temperature was 20 ± 2 °C, and the relative humidity was 65–70%. The compressive test of PCL-cement-based materials was carried out using the DW1210 electronic geotextile universal strength tester, a geosynthetic electronic strength testing machine (as shown in Fig. 6b). The loading rate was controlled by strain to 0.5 mm/min.

PCL-cement-based materials are brittle materials. According to the method standard for concrete physical and mechanical properties tests, the cubic compressive strength is defined as the stress when the specimen is broken, and the compressive modulus of elasticity is defined as the secant modulus between the starting point of an obvious straight line and the 1/3 axial compressive strength point in the stress–strain curve. The specific calculation formula is as follows:

Uniaxial compressive strength R_c :

$$R_c = \frac{P'_c}{A_0},$$

where R_c is the uniaxial compressive strength/MPa; P'_c is the load when the specimen is broken/N; A_0 is the initial cross-sectional area of the specimen/mm².

Average compressive modulus of elasticity E_{av} :

$$E_{av} = \frac{\sigma_b - \sigma_a}{\varepsilon_b - \varepsilon_a},$$

where E_{av} is the average modulus of elasticity (MPa); σ_a is the stress value at the starting point of the straight line on the relationship curve between stress and longitudinal strain; σ_b is the stress value of 1/3 of the uniaxial compressive strength; ε_a is the longitudinal strain value when the stress is σ_a ; ε_b is the longitudinal strain value when the stress is σ_b .

2.2.3 Scanning Electron Microscope Test

In scanning electron microscope (SEM), an electron beam with a certain energy bombards a solid sample to make the electrons interact with the sample, thereby generating lots of useful information, and then a special detector is used to separately collect, process and form an image. As a result, the microscopic morphology and structure of the sample can be intuitively observed. In this paper, A Hitachi S-4800 scanning electron microscope (as shown in Fig. 6c) was used to conduct scanning electron microscopy tests on the cross sections of PCL samples and PCL-cement mortar samples.

3 PCL Characteristics

3.1 Compression Deformation Characteristics of PCL Specimens

The uniaxial compression test was carried out on the granular PCL cylindrical sample. As the loading process

progressed, the sample was gradually compressed into a drum shape, and finally pressed into a pancake shape without significant fracture. Its failure pattern and characteristics were similar to those of rigid foams in compression tests, and there was no strength limit during the compression loading. In the final stage, the liquid was isolated on the surface of the material due to heating and melting. Fig. 7 shows the morphology of the granular PCL cylindrical sample before and after loading.

When loading the cubic sample of powdered PCL under the uniaxial compression, Fig. 8 shows the sample morphology when the compression ratios are 0%, 10%, 30%, and 40%, respectively. It can be seen that with the increase of the load, the cubic sample underwent a relatively obvious volumetric compression (when $h=18$ mm), and then the middle part of the sample bulged (when $h=14$ mm). During the whole loading stage, no visible tensile cracks appeared on the surface of the sample.

3.2 PCL Stress–Strain Analysis

The respective stress–strain relationship curves obtained by the uniaxial compression test on the above two forms of PCL specimens are shown in Fig. 9:

The following conclusions can be drawn from the above figure:

1. During the loading process of the granular PCL sample, when the strain is about 8%, there is a turning point, where the curve changes from steep to flat. Before this point, the stress–strain curve is approximately a straight line; after this point, the stress

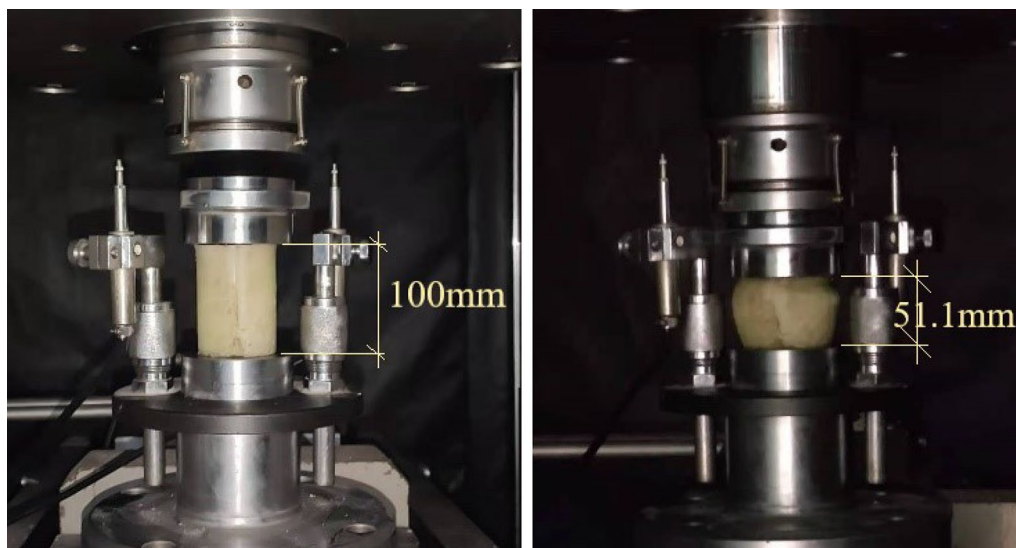
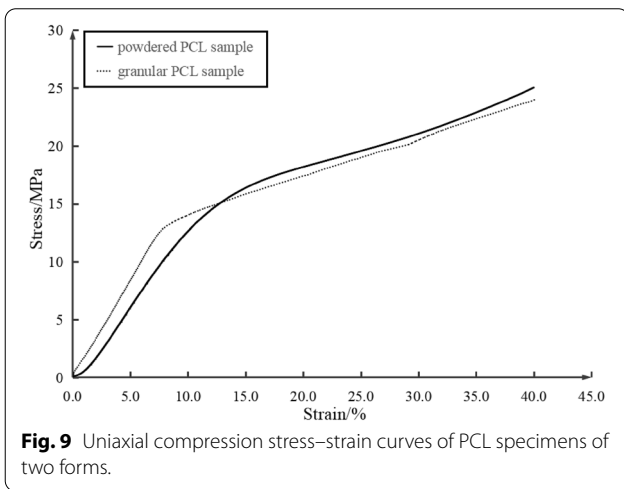
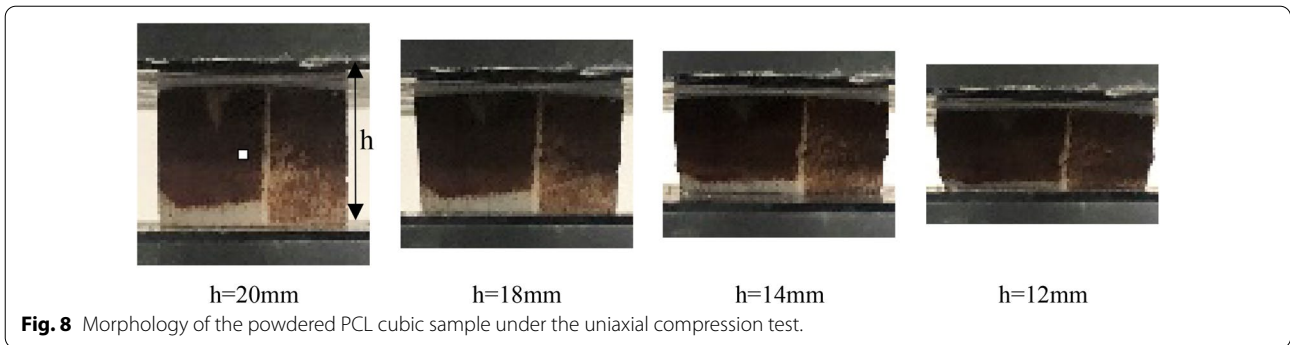


Fig. 7 Morphology of the granular PCL cylindrical sample before and after loading.



increases slowly as the strain increases. When the strain is 40%, the stress is 23.98 MPa.

2. During the loading process of the powdered PCL sample, when the strain is 12%, there is also a turning point, where the curve changes from steep to flat. When the strain reaches 40%, the stress is 25.03 MPa, showing good bearing capacity and toughness.
3. Comparing the stress–strain curves of the above two types of PCL samples, it can be found that at the initial stage of loading the linear relationship between the stress–strain curves of the granular PCL is more significant, and the stress increases faster. In the strain hardening process after the turning point, the curves of the two materials remain approximately

parallel, and the stress growth rates are basically identical.

3.3 Basic Physical and Mechanical Parameters of PCL

According to the above definition of plastic materials' compressive strength and compressive modulus of elasticity, the basic physical and mechanical properties of the sample are calculated as shown in Table 4:

3.4 Microstructure Analysis

Generally speaking, the microstructure of a material determines its macroscopic properties. To further learn the structural characteristics of PCL, the SEM observation and analysis of the PCL powder (Fig. 10) and the cross-sectional area of the PCL powder sample obtained by the melting–cooling–hardening process (Fig. 11) were performed. It can be seen from Figs. 9 and 10 that the natural aggregates of the PCL powder have irregular shapes, while the surface is relatively flat and even. The PCL powder sample obtained by the melting–cooling–hardening process has a smooth cross section, few protruding defects and no micro-cracks. The cross-sectional structure is uniform and dense, which is consistent with its excellent macroscopic mechanical properties.

4 PCL-Cement Paste Characteristics

Cement paste is often used for grouting, spray anchoring, bolt grouting, and duct grouting for prestressed concrete. The performance of cement paste plays a vital role in the

Table 4 Basic physical and mechanical parameters of PCL.

Material	Density/(g/cm ³)	Compressive strength/MPa	Compression modulus of elasticity/MPa
Granular PCL sample	1.073	13.96	165.5
Powdered PCL sample	1.086	12.57	145.2

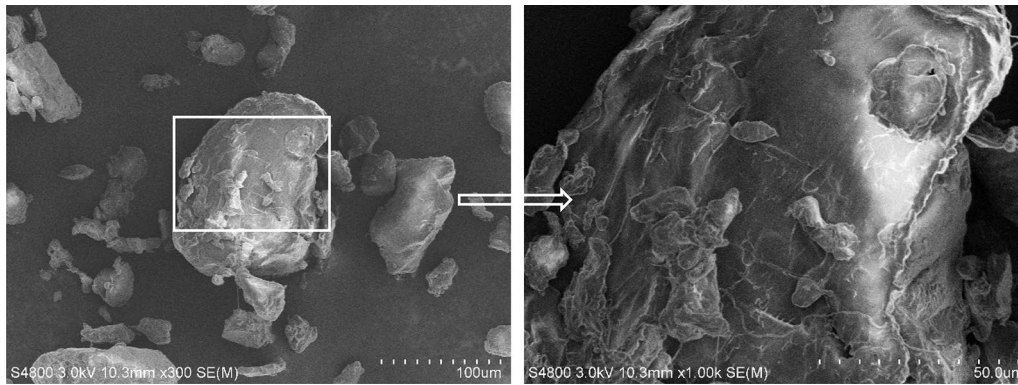


Fig. 10 SEM images of PCL powder aggregate.

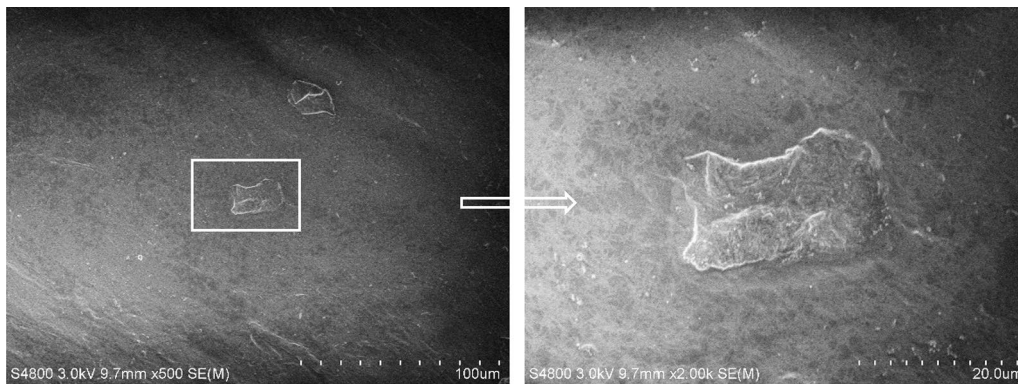


Fig. 11 SEM images of the cross-sectional area of the PCL powder sample.

anchoring effect of the anchorage section. This part of the experiment mainly studies the effect of adding PCL on the physical and mechanical properties of the cement paste. Among them, the compressive strength is the most basic mechanical performance index of cement-based materials, as it reflects the maximal load that the material can withstand.

4.1 Failure Morphology of PCL-Cement Paste Sample

A uniaxial compression test was carried out on the prepared PCL-cement paste sample, and the loading force and sample deformation amount during the loading process were monitored in real time. The shapes of the sample before and after loading are shown in Fig. 12. In the initial stage of loading, the surface of the PCL-cement paste sample was peeled off. With the increase of the load, the tensile crack developed downward from the upper end of the sample, and finally, a monoclinic

or vertical primary crack was formed, and the shear failure or tensile failure occurred.

4.2 Stress and Strain Analysis of PCL-Cement Paste

The uniaxial compression test was performed on the four sets of samples obtained through the mix design and under the preparation conditions in Table 2, and the resulting stress–strain relationship curves are shown in Fig. 13. Sample 1–1 did not mix with PCL and did not undergo a water bath heating process, but its compressive strength was the highest. It can be seen that: on the one hand, water bath heating during the initial setting of cement would significantly reduce the strength of the sample, the uniaxial compression strength would increase more slowly, and the sample would be softer throughout the deformation stage; on the other hand, as the content of PCL powder increased, the straight

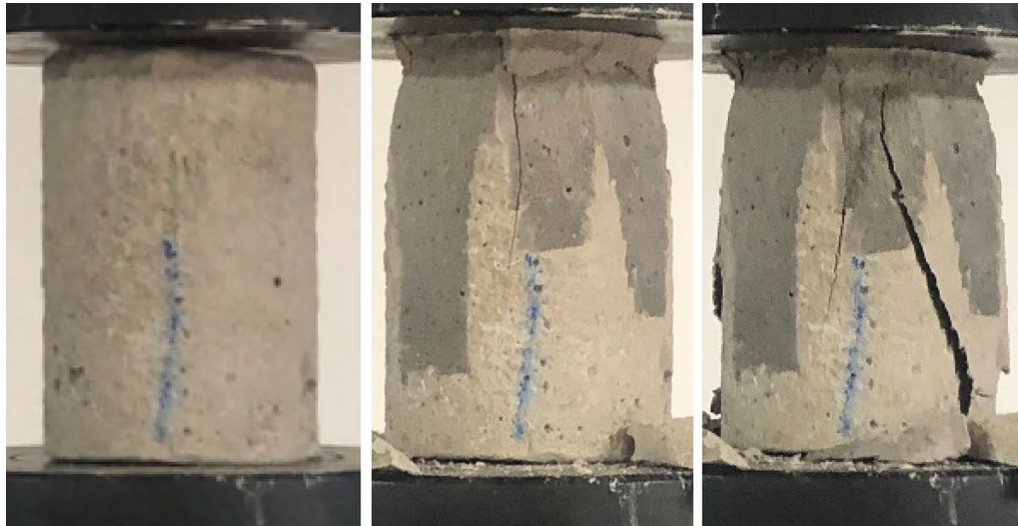


Fig. 12 Morphology of the sample before and after loading.

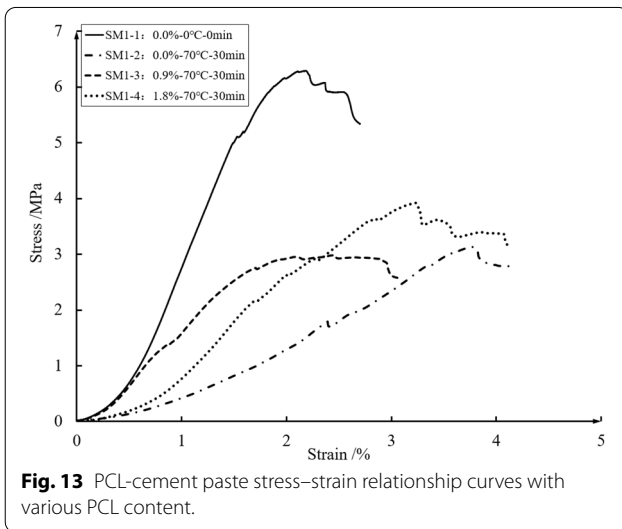


Fig. 13 PCL-cement paste stress–strain relationship curves with various PCL content.

line of the stress–strain curve became steeper, and the strength of the sample increased slightly.

4.3 Basic Physical and Mechanical Parameters of PCL-Cement Paste

The modulus of elasticity is an important index to describe the stiffness of material, and the failure strain reflects the toughness of material. Both of them can reflect the influence of PCL on the bearing capacity and deformation properties of cement paste. The basic physical and mechanical parameters of each group of samples calculated are shown in Table 5, and it can be seen that:

Water bath heating significantly reduced the compressive strength and average elastic modulus of the sample, while the failure strain was increased. Plus, the increase in the ductility of the sample also led to a decrease in strength. From the analysis of hydration mechanism, cement hydration was an exothermic process. On the one

Table 5 Mechanical properties of cement paste with various PCL content.

No.	PCL content/% (PCL/C)	Water bath temperature/°C	Water bath time/min	Maintenance cycle/d	Compressive strength/MPa	Failure strain/%	Average elastic modulus/MPa
1-1	0.0	0	0	7	6.289	1.785	461.3
1-2	0.0	70	30	7	3.134	3.193	90.1
1-3	0.9	70	30	7	2.924	2.890	185.7
1-4	1.8	70	30	7	3.921	2.613	200.0

hand, the water bath heating inhibited the progress of the hydration reaction, making the cement paste strength relatively low during the same period. On the other hand, the interior of the sample was loosen by the water bath heating, so the specimen gained better toughness while compromising strength.

At the same time, with the increase in the content of PCL, the average elastic modulus of the sample increased from 90.1 to 200.0 MPa, and the compressive strength also lifted from 3.134 to 3.921 MPa. However, the failure strain decreased from 3.193 to 2.613%, indicating that the addition of PCL can improve the strength of the cement paste.

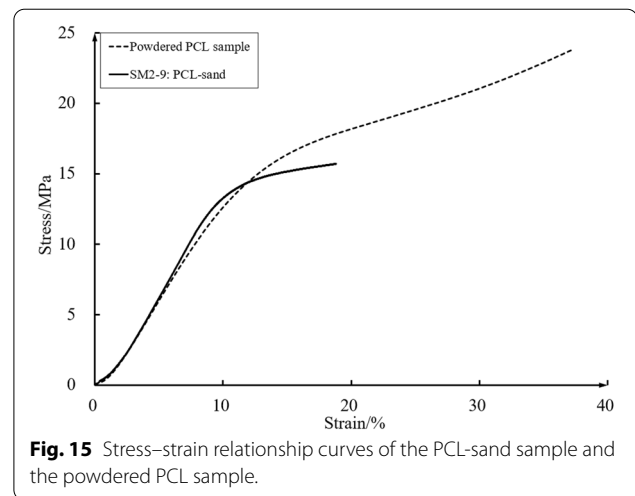
5 PCL-Cement Mortar Characteristics

Cement mortar is often used as a grouting material, a binder in masonry engineering, etc. Apart from lacking of coarse aggregate, it is identical with concrete in terms of workability, bleeding rate, strength, and shrinkage. The study of the influence of PCL content on the mechanical properties of cement mortar can reflect the bearing characteristics of grouting consolidated body under different PCL content on the one hand, and provide a reference basis for the research of PCL modified concrete on the other hand.

5.1 Physical and Mechanical Properties of PCL-Sand Sample

To study the bonding power, strength and deformation characteristics of molten PCL as a cementitious material, the experiment replaced cement with PCL as a control.

The specific mix design of the PCL-sand sample is shown in Table 3. The 20 mm cubic sample was made by water bath heating, and the uniaxial compression test was performed on it after 28 days of curing. Fig. 14 shows the sample morphology when the compression ratio is



0%, 5%, and 15%, respectively. In the early stage of loading, the morphological change of the sample was similar to that of the pure PCL powder sample. As the loading force increased, the middle part of the sample bulged; after the compression rate reached 15% ($h=17$ mm), a short vertical crack appeared in the middle of the sample. During the entire loading process, no large cracks or flaking occurred on the sample. Fig. 15 shows the comparison of the uniaxial compression stress–strain curves between the PCL-sand sample and the powdered PCL sample, and Table 6 shows the mechanical parameters of these two materials.

It can be concluded from Fig. 15 and Table 6 that:

1. The compressive strength of the PCL-sand sample is 13.26 MPa, which is slightly higher than the 12.57 MPa of the powdered PCL sample. According to the compression characteristics of plastic materials, the compressive modulus of elasticity of the PCL-sand sample is calculated to be 151.8 MPa, which is

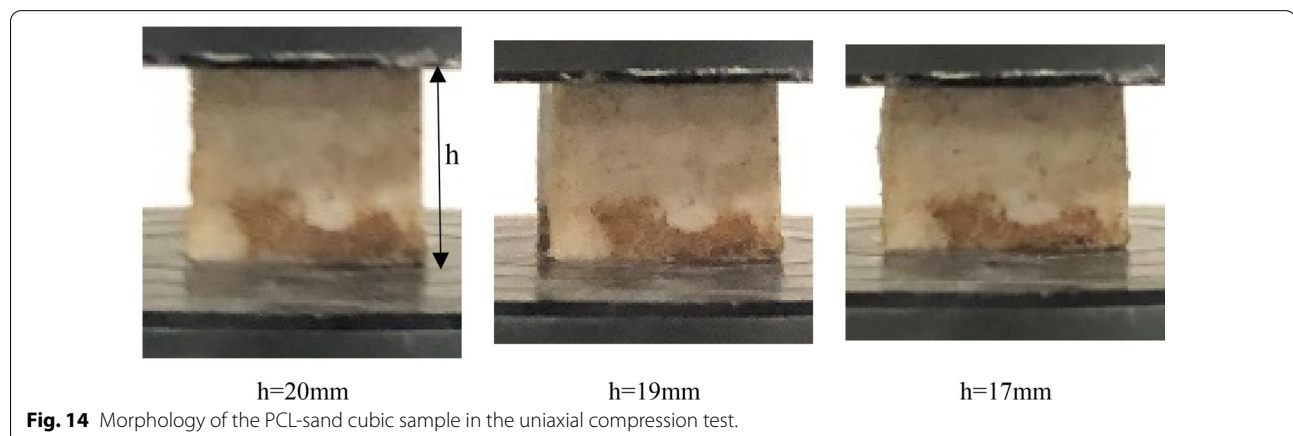
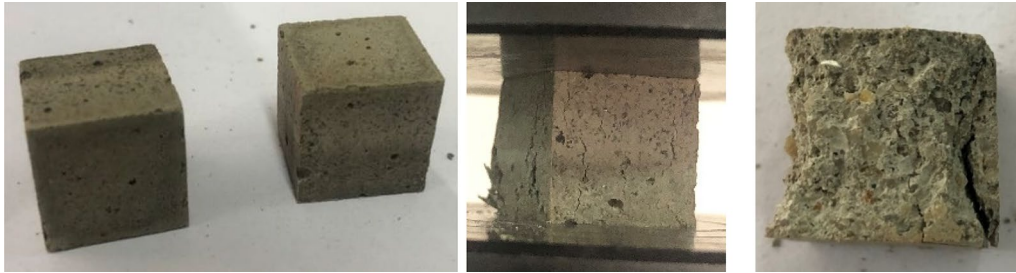


Table 6 Mechanical parameters of PCL-sand sample and the powdered PCL sample.

Sample	Ratio	Compressive strength/MPa	Compression modulus of elasticity/MPa
Powdered PCL sample	Pure PCL powder	12.57	145.2
PCL-sand sample	PCL:sand = 0.6:1	13.26	151.8

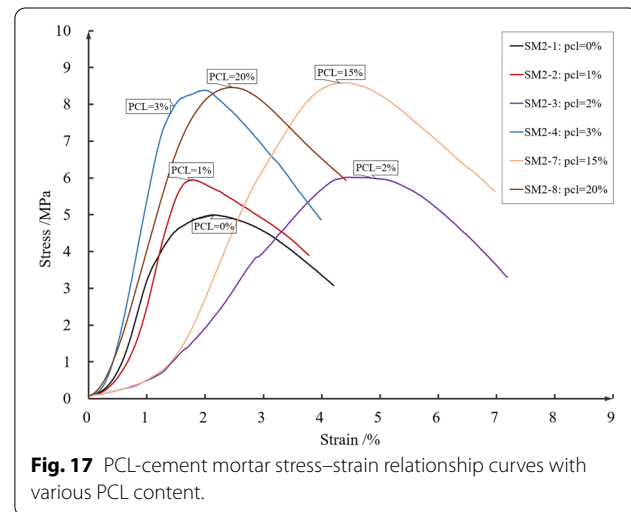
**Fig. 16** Morphology of the sample before and loading.

also slightly larger than the 145.2 MPa of the powdered PCL sample.

- At the initial loading stage, the stress–strain curves of the two materials overlap, indicating that the deformation characteristics of PCL-sand under small loads are mainly controlled by the PCL. With the further increase of the load, the PCL-sand sample yields. Since then, its strain continues to increase, but the internal stress of the sample is basically maintained at about 14 MPa. By contrast, the pure PCL sample also experiences a short yielding process, but it quickly enters the strengthening phase. As its strain continues to increase, the strength growth slows down, but there is still a significant increase. In addition, compared with ordinary silicate materials, the two specimens witness no failure and a steep curve drop during the entire loading process, and the effective strength growth can still be maintained under large compression deformation. This indicates that the use of PCL instead of cement as a cementitious material can significantly reduce the brittle deformation of cement-based materials when loaded, which is extremely beneficial to the long-term stability of the engineering project.

5.2 Failure Morphology of PCL-Cement Mortar Sample

Series uniaxial compression tests on the prepared PCL-cement mortar samples with various mix ratios were carried out. Fig. 16 shows the morphology of PCL-cement mortar sample before and after loading. It can be seen that as the loading process progresses, the surface of the

**Fig. 17** PCL-cement mortar stress–strain relationship curves with various PCL content.

sample peels off. There is an angle between the normal line of the cement mortar failure surface and the loading direction, and the failure form is X-shaped conjugate inclined plane shear failure.

5.3 Stress–Strain Analysis of PCL-Cement Mortar

Fig. 17 shows the stress–strain curves of the uniaxial compression test on cement mortar samples with different PCL content. It can be seen that, on the one hand, cement mortar with 0% PCL has the lowest strength, and its failure strain is also relatively small. The addition of PCL powder can significantly improve the strength of cement mortar. On the other hand, there is no obvious evidence to prove that PCL can improve the toughness of

Table 7 Mechanical parameters of PCL-cement mortar with various PCL content.

No.	PCL content/% (PCL/C)	Compressive strength/MPa	Failure strain/%	Average elastic modulus/%
2-1	0	4.995	2.134	2.310
2-2	1	5.946	1.802	2.178
2-3	2	6.021	4.472	0.980
2-4	3	8.383	2.009	4.090
2-5	5	4.318	5.767	0.570
2-6	10	5.771	2.617	1.965
2-7	15	8.586	4.380	2.704
2-8	20	8.462	2.483	3.591

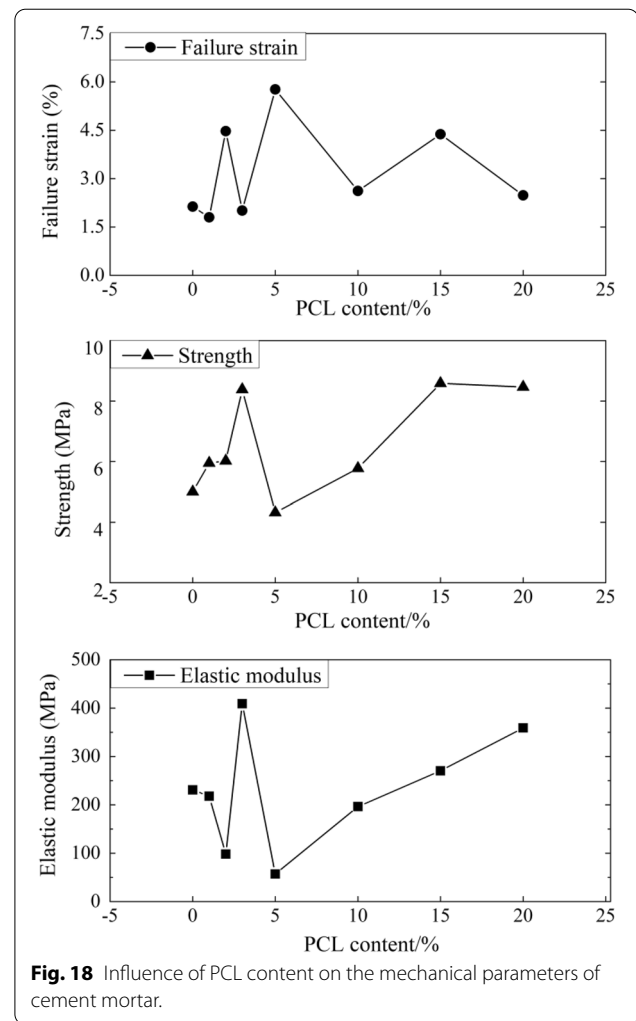
cement mortar, but it can be seen from the stress–strain relationship curves that, compared with the sample without PCL, when the PCL content is larger than 5%, both the strength and ductility of the sample can be significantly improved.

5.4 Basic Physical and Mechanical Parameters of PCL-Cement Mortar

In the process of cement-based material design and quality control, mechanical properties are the most important indicators to identify the macroscopic properties of materials, and are usually the most important properties for researchers and engineers. Calculate the compressive strength and average elastic modulus of each sample, and arrange them together with the failure strain in Table 7. At the same time, the influence of PCL content on the above three is shown in Fig. 17.

It can be concluded from Table 7 and Fig. 18 that:

1. The strength of cement mortar can be increased by adding PCL, especially when the PCL content is large ($\geq 5\%$), the strength of cement mortar is significantly improved; in this regard, we think that as an organic resin material, PCL does not participate in the hydration reaction of cement, so it only plays a role in physical modification of cement consolidated body after mixing. Combined with the SEM results, we think that when the content of PCL is small ($< 5\%$), PCL fails to form an effective stress transfer path in the consolidated body, but causes stress concentration in the sample. Thus, the cement consolidated body reaches the bearing limit earlier. When the PCL content is large ($> 5\%$), the cooling PCL floc gel may form a more stable stress release path within the sample, thus reducing the stress on the cement consolidated body, and the strength and modulus of the sample are significantly improved when the PCL con-



tent is 15%, the strength of cement mortar reaches 8.586 MPa, which is 69% higher than the 4.995 MPa of pure cement mortar.

2. By adding PCL powder, the brittleness of cement mortar can be improved to a certain extent, and the ductility of the sample can also be strengthened. It can be seen from Fig. 18 that the failure strains of the sample with PCL added are basically greater than that of the pure cement mortar, which is 2.134%. When the PCL content is 15%, the failure strain is 4.380%, which is 105% higher than that of pure cement mortar.
3. The effect of adding PCL powder on the average elastic modulus of cement mortar is not significant. When the PCL content is small, the average elastic modulus of PCL-cement mortar even decreases slightly. Only when the PCL content is greater than 15%, the average elastic modulus becomes larger than that of pure cement mortar.

5.5 Microstructure Analysis

Generally speaking, the microstructure of a material determines its macroscopic properties. On the one hand, cement mortar is a porous and multiphase material, and the micro pore structure determines the basic properties of cement mortar to a certain extent. On the other hand, the distribution of PCL powder in cement mortar directly affects the toughness, integrity and continuity of cement mortar, and is of great significance for improving the crack resistance, impermeability, impact resistance and flexibility of cement-based materials.

In this paper, PCL was added to cement mortar, and was cooled, crystallized and hardened during cement hydration. Then it intersected and clung with the cement hydration product C–S–H inside the cement, cementing the dispersed fine aggregate (sand), unhydrated cement and hydrated products to form a solid and close whole in three-dimensional space, and eventually enhancing the strength of cement stone after hardening. To understand the morphology, distribution and bonding of powdered PCL in the cement mortar, PCL-cement mortar samples

with 5% and 20% PCL were selected for SEM observation. The microscopic images are shown in Figs. 19 and 20.

It can be seen from Figs. 19 and 20 that:

1. The two cement mortar samples with different PCL content have already undergone cement hydration, forming flakes of $\text{Ca}(\text{OH})_2$ wrapped around the hydration products. At the same time, a large number of floc C–S–H growing in clusters can be observed. In Fig. 20, many micropores can be observed from the sample section, and the paste density is low, which also corresponds to the lowest strength (4.318 MPa) in uniaxial compression test.
2. It can be seen from Fig. 19 that PCL is mainly fibrous and needle-like in the cross section of the cement mortar sample, and its shape conforms to the characteristics of ductile materials when there is tensile failure. At the same time, fibrous PCL is more concentrated in the cement hydration products by embedding in the C–S–H gel, but is less distributed in the area of unhydrated cement or fine aggregates

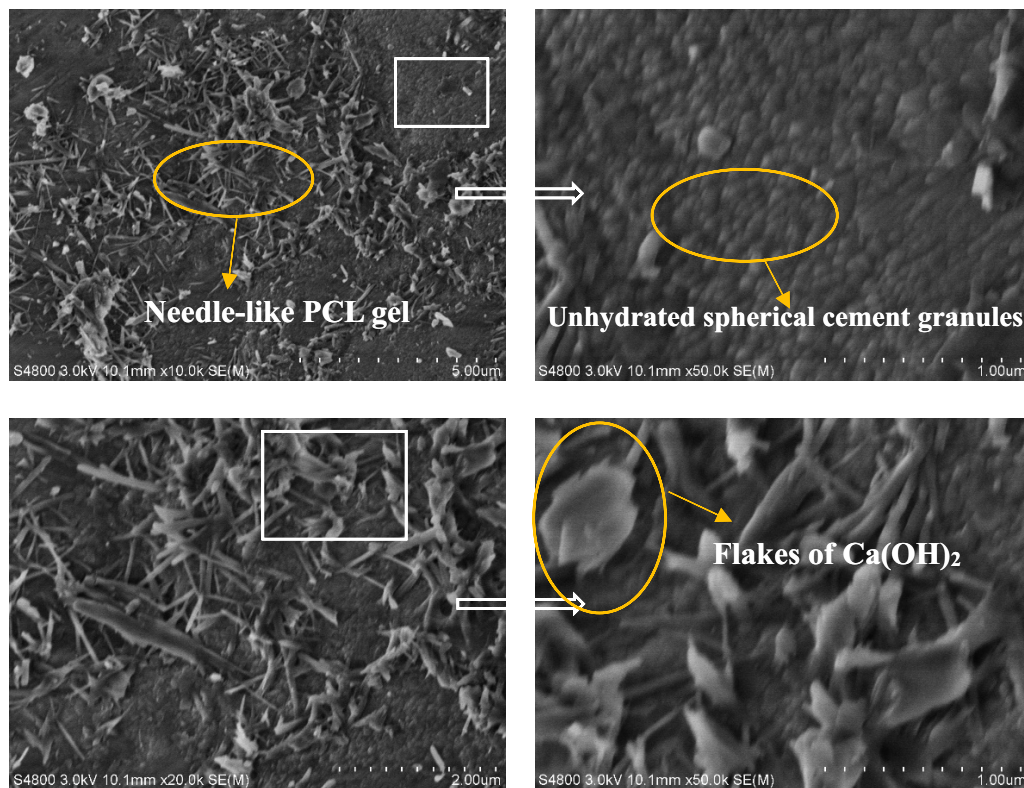


Fig. 19 SEM image of PCL-cement mortar cross section (PCL = 20%).

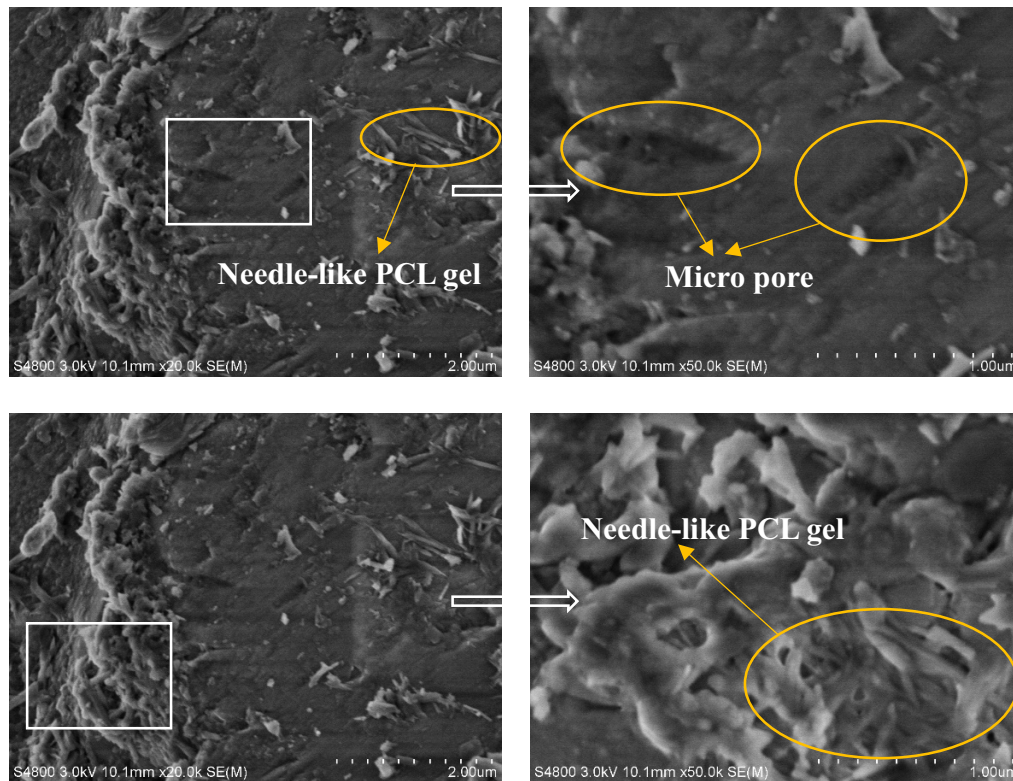


Fig. 20 SEM image of PCL-cement mortar cross section (PCL = 5%).

(sand particles). In Fig. 20, the PCL fiber observed in cement mortar with less PCL content is significantly reduced.

6 Summary

By studying the properties of PCL, a high ductility material, we creatively adds molten PCL powder to cement-based paste, and examines in-depth the physical and mechanical properties and the microstructure characteristics of cement pastes and cement mortars with different PCL content. The conclusions are as follows:

1. PCL has good ductility and compressive strength, and its strength is relatively high in the early stage of compression. After 24 h of curing, its strength is greater than 12 MPa. When adding 0.0%, 0.9%, and 1.8% PCL into the cement paste to make a standard sample for uniaxial compression test, it is found that with the increase of PCL content, the compressive strength of cement paste sample has been significantly improved, but the failure strain has decreased. This may be caused by the relatively small content of PCL.
2. The PCL-sand sample prepared with PCL as the cementitious material has similar load-bearing characteristics to pure PCL powder at the initial stage of compression. At the end of the loading stage, there is a yield phenomenon but no brittle fracture, showing good ductility and high strength. When adding 1%, 2%, 3%, 5%, 10%, 15%, 20% PCL into the cement mortar, it is found that when the PCL content is higher (greater than 15%), the strength and ductility of cement mortar can be significantly improved.
3. Through the SEM observation of the powdered PCL sample, it is found that the internal structure of the sample is uniform and compact, and there is no micro-crack after compression. This demonstrates that PCL has good toughness and high strength from a macroscopic perspective. At the same time, through the SEM observation of the cross section of cement mortar samples with PCL content of 5% and 20%, respectively, we have found fibrous or needle-like PCL powder embedding in the cement base or the pores of the C-S-H gel, making the structure of the cement mortar even denser. Therefore, it can be proved that the addition of PCL has enhanced the strength and reduce the brittleness of the traditional cement mortar.

4. The current research merely focuses on PCL modified cement paste and cement mortar for grouting reinforcement materials. In the future, we may further study the mechanical properties of PCL modified concrete, so as to provide basis for high-strength and high-performance design of concrete.

Acknowledgements

The first author gratefully acknowledges the support from Laboratory of deep rock mechanics, Wuhan University.

Authors' contributions

HL designed the experiment and analyzed the main points. KZ was a major contributor in testing and writing the manuscript. JY and AW helped doing test and data examination. All authors read and approved the final manuscript.

Authors' information

Hai-feng Lu, Associate Professor, School of civil engineering and architecture, Whuhan University, Wuhan, 430072, China. Kai Zhang, Master Student, School of civil engineering and architecture, Whuhan University, Wuhan, 430072, China. Jin-long Yi, Master Student, School of civil engineering and architecture, Whuhan University, Wuhan, 430072, China. Ai-chao Wei, Master Student, School of civil engineering and architecture, Whuhan University, Wuhan, 430072, China.

Funding

The research is supported by the Key R & D projects in Hubei Province 2021BAA059 and Natural Science Foundation of China under project 51974203.

Availability of data and materials

All data, models, and code generated or used during the study appear in the submitted article. The data sets used and/or analyzed during the current study are available from the corresponding author on reasonable request.

Declarations

Ethics approval and consent to participate

Not applicable.

Consent for publication

All authors of the manuscript have read and agreed to its content and are accountable for all aspects of the accuracy and integrity of the manuscript in accordance with ICMJE criteria.

Competing interests

The authors declare that they have no competing interests.

Author details

¹School of Civil Engineering, Wuhan University, Wuhan 430072, Hubei, China.

²Hubei Key Laboratory of Geotechnical and Structural Engineering Safety, Wuhan University, Wuhan 430072, Hubei, China.

Received: 20 November 2021 Accepted: 23 February 2022

Published online: 10 May 2022

References

- Abbah, S. A., Lam, C. X., Huttmacher, D. W., et al. (2009). Biological performance of a polycaprolactone-based scaffold used as fusion cage device in a large animal model of spinal reconstructive surgery. *Biomaterials*, *30*(28), 5086–5093.
- Ajili, S. H., Ebrahimi, N. G., & Soleimani, M. J. A. B. (2009). Polyurethane/polycaprolactone blend with shape memory effect as a proposed material for cardiovascular implants. *Acta Biomaterialia*, *5*(5), 1519–1530.
- Alani, A., Knowles, J. C., Chrzanowski, W., et al. (2009). Ion release characteristics, precipitate formation and sealing ability of a phosphate glass-polycaprolactone-based composite for use as a root canal obturation material. *Dental Materials: Official Publication of the Academy of Dental Materials*, *25*(3), 400–410.
- Barton, N., & Choubey, V. (1977). The shear strength of rock joints in theory and practice. *Rock Mechanics*, *10*(1), 1–54.
- Bruce, D. A., Naudts, A., & Gause, C. (1999). Rock grouting: Contemporary concepts in materials, methods, and verification. *Geo-engineering for underground facilities* (pp. 936–949). ASCE.
- Chen, T., Cai, T., Jin, Q., & Ji, J. (2015). Design and fabrication of functional polycaprolactone. *E-Polymers*, *15*(1), 3–13.
- Du, M. R. (2018). *Mechanical properties and micro action mechanism of carbon nanotube reinforced cement-based grouting materials*. China University of Mining and Technology.
- Du, M. R., Jing, H. W., Su, H. J., Zhu, T. T., & Chen, M. L. (2017). Strength and failure characteristics of sandstone containing two circular holes filled with two types of inclusions under uniaxial compression. *Journal of Central South University*, *24*(11), 2487–2495.
- Guan, X., Zhang, H. B., Yang, Z. P., Li, H. Y., Lu, J. J., Di, H. F., & Wang, G. P. (2020). Research of high performance inorganic-organic composite grouting materials. *Journal of China Coal Society*, *45*(3), 902–910.
- Han, X., Zhu, Q., Cheng, C., & Wu, C. (2011). Homogeneous synthesis and characterization of graft copolymer of chitosan/polycaprolactone. *CIESC Journal*, *62*(7), 2055–2060.
- Kumar, C. S., Soloman, A. M., Thangam, R., Gopinath, A., & Madhan, B. (2020). Ferulic acid-loaded collagen hydrolysate and polycaprolactone nanofibres for tissue engineering applications. *IET Nanobiotechnology*, *14*(3), 202–209.
- Leonés, A., Mujica-García, A., Arrieta, M. P., Kenny, J. M., & Peponi, L. (2020). Organic and inorganic PCL-based electrospun fibers. *Polymers*, *12*(6), 1325.
- Li, F., Shi, Y., Li, P., & Jiang, T. (2020). Research progress of ring-opening polymerization of ε-caprolactone initiated by degradable biopolymers. *Current Organic Chemistry*, *24*(13), 1507–1516.
- Li, G. L., & Zhu, Y. Q. (2008). Large deformation control technology of high ground stress weak surrounding rock of Wushaoling Tunnel. *Journal of Railway Engineering*, *03*, 54–59.
- Li, S., Xu, F., Li, L., Wang, W. M., Zhang, W., Zhang, Q. Q., & Shi, S. S. (2016). State of the art: Challenge and methods on large deformation in tunnel engineering and introduction of a new type supporting system. *Chinese Journal of Rock Mechanics and Engineering*, *35*(7), 1366–1376.
- Li, W., Kang, H., Jiang, Z., Cai, R., & Guo, G. (2021). Deformation failure mechanism of fractured deep coal-rock mass and high-pressure grouting modification strengthening testing. *Journal of the China Coal Society*, *46*(3), 912–923.
- Liu, Q. S., Deng, P. H., Bi, C., Li, W. W., & Liu, J. (2019). FDEM numerical simulation of the fracture and extraction process of soft surrounding rock mass and its rockbolt-shotcrete-grouting reinforcement methods in the deep tunnel. *Rock and Soil Mechanics*, *40*(10), 4065–4083.
- Liu, Z. C., Zhu, Y. Q., Li, W. J., & Liu, P. X. (2008). Mechanism and classification criterion for large deformation of squeezing ground tunnels. *Chinese Journal of Geotechnical Engineering*, *30*(5), 690–697.
- Lu, H. F., Zhu, C. D., & Liu, Q. S. (2021). Study on shear mechanical properties of structural planes grouted with different materials. *Journal of Rock Mechanics and Engineering*, *40*(9), 1803–1811.
- Qing, P. F., Wang, W. L., & Yuan, Y. (2021). Study on grouting technology and its application in geotechnical engineering. *Geology and Exploration*, *57*(03), 631–639.
- Sha, P., Wu, F. Q., Li, X., Liang, N., & Chang, J. Y. (2015). Squeezing deformation in layered surrounding rock and force characteristics of support system of a tunnel under high in-situ stress. *Rock and Soil Mechanics*, *36*(5), 1407–1414.
- Wang, H. X., Zhang, G. Z., Ding, Q. J., Hu, S. G., Tan, S. H., & Li, Y. J. (2007). Research on the performance of double solution grouting material with alkali-activated industry waste slag. *Jianzhu Calliao Xuebao (Journal of Building Materials)*, *10*(3), 374–378.
- Woodruff, M. A., & Huttmacher, D. W. (2010). The return of a forgotten polymer—Polycaprolactone in the 21st century. *Progress in Polymer Science*, *35*(10), 1217–1256.

- Yang, H. L. (2009). *Deformation and reinforcement mechanism of fractured rock mass under grouting and its application*. Shandong University.
- Zhao, W. H., Jin, H. W., Su, H. J., & Li, D. (2015). Strength and fracture characteristics of sandstone containing coplanar fissure group. *Engineering Mechanics*, 32(2), 183–189.

Publisher's Note

Springer Nature remains neutral with regard to jurisdictional claims in published maps and institutional affiliations.

Submit your manuscript to a SpringerOpen[®] journal and benefit from:

- ▶ Convenient online submission
- ▶ Rigorous peer review
- ▶ Open access: articles freely available online
- ▶ High visibility within the field
- ▶ Retaining the copyright to your article

Submit your next manuscript at ▶ [springeropen.com](https://www.springeropen.com)
